Heliyon 10 (2024) e34352

Contents lists available at ScienceDirect

Heliyon

journal homepage: www.cell.com/heliyon

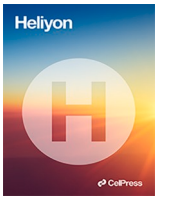

Research article

Bile acid metabolism modulates intestinal immunity involved in ulcerative colitis progression

Hua Huang [a], Shuai Yan [b,1], Tianwei Guo [c], Qiuwen Hua [d], Yongtong Wang [a], Shanshan Xu [e,**], Lijiang Ji [a,*]

[a] *Department of Anorectal Surgery, Changshu Hospital Affiliated to Nanjing University of Chinese Medicine, Changshu, 215500, Jiangsu Province, China*
[b] *Department of Anorectal Surgery, Suzhou TCM Hospital Affiliated to Nanjing University of Chinese Medicine, Suzhou, 215000, Jiangsu Province, China*
[c] *Department of Pathology, Changshu Hospital Affiliated to Nanjing University of Chinese Medicine, Changshu, 215500, Jiangsu Province, China*
[d] *Department of Digestive System, Changshu Hospital Affiliated to Nanjing University of Chinese Medicine, Changshu, 215500, Jiangsu Province, China*
[e] *Department of Anorectal Surgery, Nantong Hospital of Traditional Chinese Medicine, Nantong Hospital Affiliated to Nanjing University of Chinese Medicine, Nantong, 226000, Jiangsu Province, China*

A R T I C L E I N F O

Keywords:
Bile acid metabolism
Immunity
Ulcerative colitis

A B S T R A C T

The bile acids (BA) in the intestine promote inflammation by interacting with immune cells, playing a crucial role in the progression of UC, but the specific mechanism between the two remains elusive. This study aims to explore the relationship between BAMand UC inflammation and determine its potential mechanisms.Firstly, we employed a hybrid approach using Lasso regression and support vector machine (SVM) feature selection in bioinformatics to identify genes linked to UC and BAM. The relationship between these genes and immune infiltration was explored, along with their correlation with immune factors in the Tumor-Immune System Interaction Database (TISIDB) database. Gene Set Enrichment Analysis (GSEA) pathway enrichment analysis was then used to predict signaling pathways associated with key genes in UC. Single-cell data from the GSE13464 dataset was also analyzed. Finally, Five differentially expressed genes (DEGs) related to BAM (APOA1, AMACR, PEX19, CH25H, and AQP9) were significantly upregulated/downregulated in UC immune cells. The expression of important genes in UC tissue was confirmed in the experimental validation section and AQP9, which showed significant differential expression, was chosen for further validation. The results showed that the AQP9 gene may regulate the IFN - γ/JAK signaling axis, thereby promoting CD8+T cell activation. This research has greatly advanced our comprehension of the pathogenesis and underlying mechanism of BAM in immune cells linked to UC.

* Corresponding author.
** Corresponding author.
E-mail addresses: symphoni33@163.com (S. Xu), fsyy01040@njucm.edu.cn (L. Ji).
[1] Contributed equally.

https://doi.org/10.1016/j.heliyon.2024.e34352
Received 2 April 2024; Received in revised form 7 July 2024; Accepted 8 July 2024
Available online 14 July 2024

1. Introduction

Ulcerative colitis (UC) is a chronic non-specific inflammatory disease of unknown etiology primarily affecting the colorectal mucosa and submucosa. Its protracted duration and propensity for recurrence can significantly impact the quality of life of individuals, potentially elevating the likelihood of developing colitis-associated neoplasms [1,2]. Currently, the etiology and pathophysiological mechanisms of UC are yet to be fully elucidated, with potential associations with genetic, environmental, microbial, and inflammatory factors [3]. Specifically, aberrations in the intestinal immune system are directly implicated in the disease onset. Common therapeutic approaches for UC management encompass aminosalicylic acid preparations, antibiotics, corticosteroids, biologics, and probiotics [4]. Nevertheless, these interventions may provide only partial symptom relief and are linked to notable adverse effects [5]. Hence, there is an urgent need to identify novel drug targets and formulate potent and safe pharmaceutical agents for the management of UC.

Immune system dysfunction is the most important promoting factor for UC [6]. Neutrophils, such as helper T cell-17 (Th17) and natural killer cells (NK), and their released cytokines, have been shown to infiltrate the intestinal mucosa of UC patients [7]. Interleukin (IL) is an important member of cytokines, involved in many cellular and tissue immune responses [8]. Toll like receptors (TLRs) are widely distributed in various cells and can recognize molecules expressed by pathogens, playing an important role in connecting innate and adaptive immunity [9], further suggesting that immunity plays a pivotal role in UC [10].

The differentiation and function of immune cells may be regulated by gut microbiota metabolites such as short chain fatty acids (SCFAs) and bile acid (BA) derivatives [11]. BA and its derivatives can bind to nuclear receptors and cell surface receptors expressed in various immune cells, including Macs, DCs, myeloid-derived suppressor cells (MDSCs), regulatory T cells (Tregs), regulatory B cells (Bregs), innate lymphoid cells (ILCs), Th17 cells, $CD4^+$ Th1 cells, Th2 cells, CD8 cells, B cells and natural killer T (NKT) cells. These BAs and their derivatives can affect the differentiation and function of these immune cells in distinct manners [12]. BA can stimulate the proliferation of intestinal stem cells (ISCs) and is an important regulatory substance for the integrity of intestinal epithelial barrier function, closely related to immune homeostasis [13]. However, the potential immune mechanism by which BAM affects intestinal barrier function is still unclear. Utilizing the GSE42911 dataset, derived from the Affymetrix microarray platform, the present study sought to explore the etiology of UC and offer innovative perspectives for its timely detection and the advancement of pharmacological treatments.

2. Materials and methods

2.1. Dry lab

2.1.1. Retrieval of datasets

The Gene Expression Omnibus (GEO) database (https://www.ncbi.nlm.nih.gov/geo/info/datasets.html), maintained by the National Center for Biotechnology Information (NCBI) in the USA, serves as a repository for gene expression data. Specifically, the GSE75214 dataset was accessed from the GEO database, using the GPL6244 annotation platform. This dataset included 96 samples in total, with 22 being healthy controls and 74 UC samples. Additionally, the GSE87473 dataset was also sourced from the GEO database, utilizing the GPL13158 annotation platform. This dataset consisted of 127 samples, including 21 healthy controls and 106 UC samples. Moreover, single-cell data files for GSE134649 were obtained from the NCBI GEO database, selecting 6 samples with comprehensive expression profiles for analysis.

2.1.2. Difference analysis

The limma package [14], an R package tailored for differential expression analysis, is widely utilized for identifying significantly differentially expressed genes between groups. In this study, the R package "limma" was applied to investigate the molecular mechanisms in UC data. It was specifically used to detect differentially expressed genes between control and disease samples. The criteria for identifying differential genes included a P value < 0.05 and a log fold change (FC) > 0.585. Moreover, volcano plots and heatmaps were generated to visually represent the differential gene expression results.

2.1.3. Function enrichment analysis

The intersection genes were functionally annotated using the Cluster Profiler [15] tool to thoroughly understand their functional significance. Gene Ontology (GO) and the Kyoto Encyclopedia of Genes and Genomes (KEGG) were utilized to evaluate the pertinent functional categories. Pathways showing significant enrichment in both GO and KEGG, with p-values and q-values under 0.05, were identified as significant categories.

2.1.4. The feature selection process of lasso regression and SVM algorithm

We utilized Lasso logistic regression and the SVM algorithm [16] for selecting diagnostic markers of the disease. The Lasso algorithm was executed using the "glmnet" package [17] in R. Furthermore, SVM-RFE, a machine learning technique based on support vector machines, was employed to identify the most predictive variables by removing feature vectors produced by SVM. SVM-RFE models were constructed using the "e1071" software package to further assess the diagnostic value of these biomarker pairs.

2.1.5. Immunoassay

The CIBERSORT [18] method is a popular technique for assessing immune cell types within the microenvironment. This approach is based on support vector regression and conducts deconvolution analysis on the expression matrix of immune cell subtypes. It

includes 547 biomarkers that differentiate 22 human immune cell phenotypes, such as T cells, B cells, plasma cells, and myeloid cell subsets. In this study, the CIBERSORT algorithm was employed to analyze patient data, aiming to estimate the relative proportions of 22 infiltrating immune cell types. Additionally, Pearson correlation analysis was performed to evaluate the relationship between gene expression and immune cell content.

2.1.6. GSEA pathway enrichment analysis

Gene Set Enrichment Analysis (GSEA) [19] employs a predefined gene set to rank significant genes based on their differential expression between two sample types. It then determines if the specified gene set is enriched at the top or bottom of the ranked list. In this study, GSEA was used to compare the differences in the KEGG signaling pathways between the high expression and low expression groups. The objective was to elucidate the molecular mechanisms underlying the core genes of the two patient groups. The analysis was conducted with 1000 permutations, and the permutation type was set to phenotype.

2.1.7. The key transcriptional genes

The R package RcisTarget [20] was used for predicting transcription factors. RcisTarget's calculations are based on motifs. The normalized enrichment score (NES) of a motif depends on the total number of motifs present in the database. In addition to motifs annotated with source data, additional annotations were inferred based on motif similarity and gene sequences. To estimate the overexpression of each motif within a gene set, the area under the curve (AUC) for each motif-motif set pair was calculated. This involved computing the recovery curve of the gene set against the motif ordering. Subsequently, the NES for each motif was determined from the AUC distribution of all motifs in the gene set.

2.1.8. Single cell analysis

Initially, the data was processed using the Seurat package [21], and the positional relationships between clusters were determined through t-distributed stochastic neighbor embedding (tSNE) algorithm analysis. Next, clusters were annotated with the celldex package, focusing on cells that were critical to disease pathogenesis. Finally, marker genes for each cell subtype were extracted from the single-cell expression profile by setting the logfc.threshold parameter of FindAllMarkers to 1. Genes with $|\text{avg log2FC}| > 1$ and p-value adj < 0.05 were identified as unique marker genes within each cell subtype.

2.1.9. Wet lab

Meanwhile, we employed reverse transcription-polymerase chain reaction (RT-PCR) and Western blot techniques to assess the expression of key genes in UC tissue and the pathway in $CD8^+$ T cell line CTLL2.

2.1.10. Animal tissue acquisition

Male (20–25 g) C57BL/6 mice (n = 20) were purchased from Beijing Sibeifu Experimental Animal Technology Co., Ltd. All mice were placed SPF grade experimental animals at room temperature (25 ± 2 °C), with a light/dark cycle of 12/12 h, and were fed freely on a standard diet. All animal experiments were approved by the Animal Ethics Committee of Nanjing University of Chinese Medicine. The mice were randomly divided into two groups. The model group was treated with drinking water containing 2.5 % DSS for 7 days to construct a colitis model, while the control group was treated with the same volume of PBS. Immediately after anesthesia, the mice were euthanized, and colon tissue was taken and stored at −80 °C.

2.1.11. Cell culture

The CD8+T cell line CTLL2 was cultured in complete Roswell Park Memorial Institute (RPMI) 1640 growth medium containing 10 % (v/v) fetal bovine serum (FBS), 50 μ M 2-mercaptoethanol, and 100 units/ml of recombinant human IL-2 protein, and passaged every 2–3 days [22]. The cells were treated with 10 ng/mL of TNF-α for a duration of 4 h.

Table 1
The primers of RT-PCR.

Gene	Primer	Sequences(5′-3′)
Apoa1	F	GGCACGTATGGCAGCAAGAT
	R	CCAAGGAGGAGGATTCAAACTG
Amacr	F	GCCAATCGGGAATTTTCTCCA
	R	GTAGGGGTTCTCACCGCTT
Pex19	F	GACAGCGAGGCTACTCAGAG
	R	GCCCGACAGATTGAGAGCA
Ch25 h	F	TGCTACAACGGTTCGGAGC
	R	AGAAGCCCACGTAAGTGATGAT
Aqp9	F	TGGTGTCTACCATGTTCCTCC
	R	AACCAGAGTTGAGTCCGAGAG
β-actin	F	GGCTGTATTCCCCTCCATCG
	R	CCAGTTGGTAACAATGCCATGT

2.1.12. Western blot

Western blotting was utilized to assess the expression of apolipoprotein A1 (APOA1), alpha-methylacyl-CoA racemase (AMACR), peroxisomal biogenesis factor 19 (PEX19), cholesterol-25-hydroxylase (CH25H), aquaporin-9 (AQP9), IFN-γ, Janus kinase (JAK), and apoptosis-related genes B-cell lymphoma 2 (Bcl2), and Bcl2-associated X protein (BAX). The secondary antibodies are donkey anti rabbit IRDye800 and donkey anti mouse IRDye680 secondary antibodies, imaged using the Odyssey imaging system. Quantify protein bands using ImageStudioLite software.

2.1.13. Real time PCR

Use RT-PCR to detect the mRNA expression of target genes. Mouse CD8+T cells were pretreated with carrier control (dimethyl sulfoxide (DMSO)) or 10 ng/mL TNF - α for 24 h. Total RNA was extracted using RNeasy Mini kit, complementary DNA (cDNA) was synthesized, and detected on QuantStudio 5 real-time PCR instrument according to the reaction system.The primers used are listed in Table 1.

2.1.14. Statistical analysis

All statistical analyses were performed using R language (Version 4.2.2), and $P < 0.05$ was considered statistically significant.

3. Results

3.1. Gene diversity related to BAM in UC

GSE75214 and GSE87473 datasets related to UC were downloaded from the GEO database, encompassing expression profile data from 223 patient groups, including the control group (n = 43) and the disease group (n = 180). The state vector algorithm (SVA) was utilized to correct the chips, and a principal component analysis (PCA) plot was employed to illustrate the batch situation pre- and post-correction. The SVA algorithm successfully mitigated the batch effect across chips (Supplementary Figure). The limma package was utilized to calculate differentially expressed genes (DEGs) between the control and disease groups. The screening criteria were set as *P*-value < 0.05 and logFC > 0.585, resulting in the identification of 2,318 DEGs, including 1,211 upregulated and 1,107 down-regulated genes (Fig.1A-B). Subsequently, the 2,318 DEGs were intersected with BAM-related genes, yielding 35 overlapping DEGs (Fig. 1C). Pathway analysis of the overlapping genes was further conducted. GO enrichment analysis revealed that the overlapping

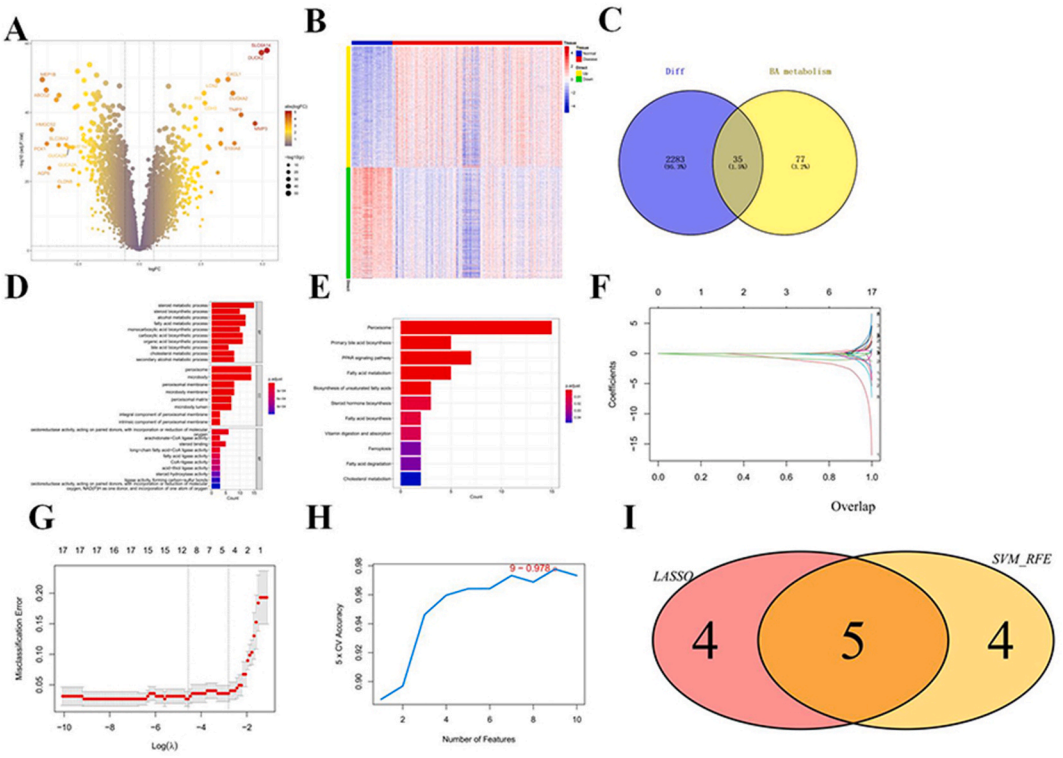

Fig. 1. The differential gene related to BAM and key genes affecting UC. A: The volcano of differential gene; B: The volcano of differential gene; C: The venn of differential gene; D: The pathway analysis on the intersection genes. The GO enrichment analysis; E: The KEGG enrichment analysis; F: Lasso regression; G: The volcano of selection algorithm; H: The venn of UC by the SVM-RFE algorithm; I: The c-lasso-SVM-venn of the characteristic genes.

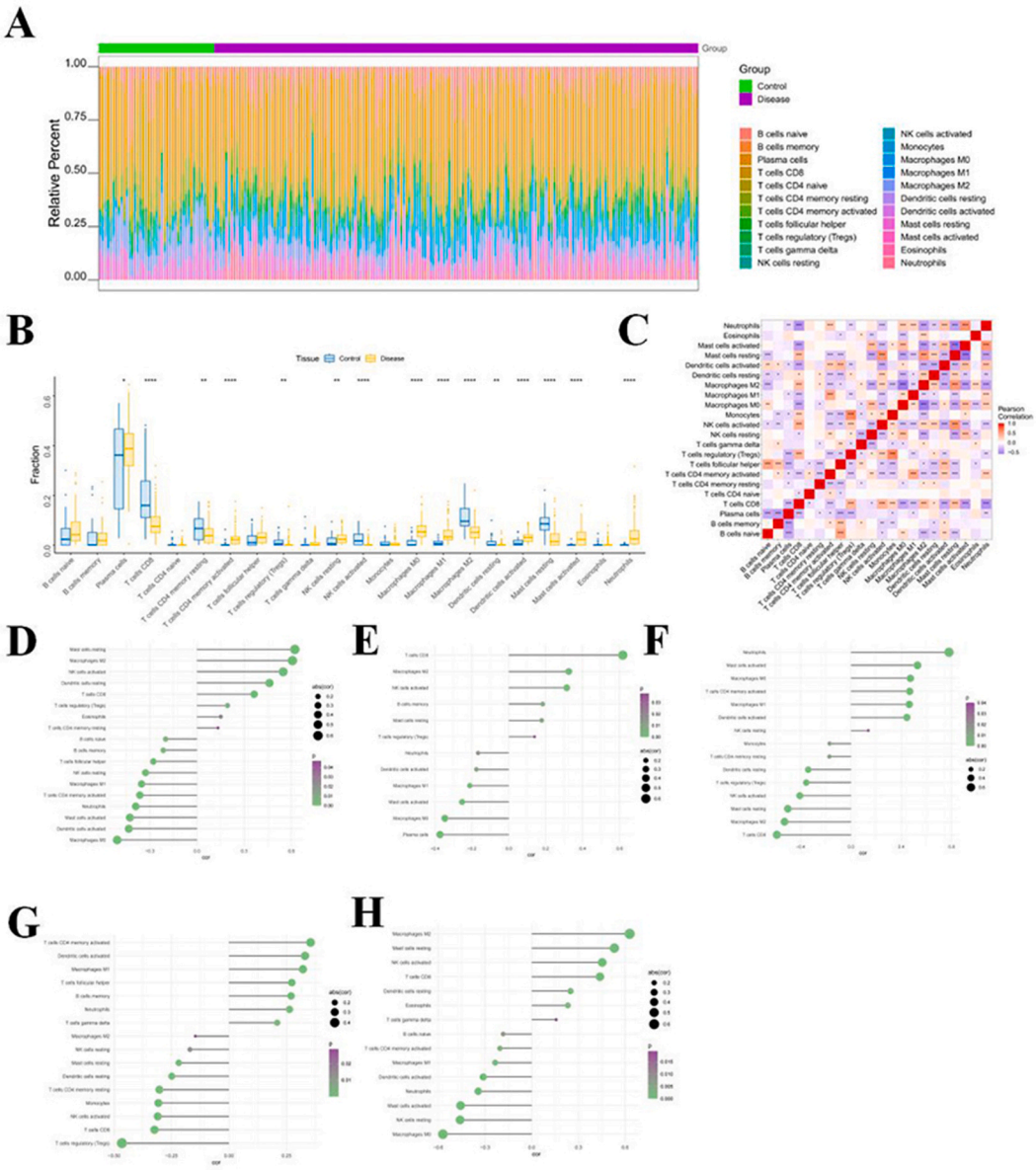

Fig. 2. The microenvironment related to the five key genes. A: Immune infiltration; B: Immune cell correlation map; C: Immune cell comparison. D: Correlation between cibersort and expression of AMAC; E: Immune infiltration Correlation between cibersort and expression of APOA1; F: Immune infiltration Correlation between cibersort and expression of AQP9; G: Immune infiltration Correlation between cibersort and expression of CH25H; H: Immune infiltration Correlation between cibersort and expression of PEX19.

genes were primarily enriched in signaling pathways such as steroid metabolic process and peroxisome. Additionally, KEGG pathway enrichment analysis demonstrated that the genes were primarily enriched in the PPAR signaling pathway, fatty acid metabolism, fatty acid biosynthesis, and other signaling pathways (Fig. 1D–E).

To further identify the key genes that affecsupportt UC, a combination of the least absolute shrinkage and selection operator (LASSO) regression and support vector machine (SVM) feature selection algorithms was employed to screen for intersectional DEGs (Figs. 1F-G). Additionally, signature genes in UC were evaluated using the SVM-recursive feature elimination (RFE) algorithm (Fig. 1H). The top 9 characteristic genes in the UC dataset exhibited the highest accuracy (Fig. 1I). Based on these findings, 5 intersection genes, including APOA1, AMACR, PEX19, CH25H, and AQP9, were identified as the key genes for subsequent analysis.

3.2. The microenvironment affecting UC

A microenvironment, composed primarily of immune cells, extracellular matrix, various growth factors, inflammatory factors, and

distinct physical and chemical characteristics, significantly impacts the diagnosis, survival outcome, and clinical treatment sensitivity of diseases. Subsequently, the relationship between the five key genes and immune infiltration was analyzed to further investigate the potential molecular mechanism by which the key genes influence UC progression. The distribution of immune infiltration levels and the heat map of immune cell correlations are presented in Fig. 2A–B. Compared with normal patients, UC patients exhibited significantly increased levels of plasma cells, activated memory $CD4^+$ T cells, resting NK cells, M0 macrophages, M1 macrophages, activated DCs, activated mast cells, and neutrophils (Fig. 2C). Furthermore, all five key genes were strongly correlated with immune cells (Fig. 2D–H), aligning with our expectations.3.4 Relationship between the five key genes and different immune factors and pathway.

3.3. Relationship between five key genes and different immune factors and pathway

Additionally, correlations between the five key genes and various immune factors were obtained from the TISIDB database [23], encompassing immune-related chemokines, immunosuppressants, immune stimulators, receptors, etc. (Fig. 3A–E). These analyses indicated that the key genes were intricately associated with the degree of immune cell infiltration and played crucial roles in the immune microenvironment.

The current study further attempted to investigate the specific signaling pathways linked to the five key genes and clarify the molecular mechanisms by which these genes influence the progression of UC. The GSEA results revealed that AMACR was enriched in signaling pathways such as CYTOSOLIC_DNA_SENSING_PATHWAY, BETA_ALANINE_METABOLISM, and JAK_-STAT_SIGNALING_PATHWAY (Fig. 3F); APOA1 was enriched in TYROSINE_METABOLISM, PHENYLALANINE_METABOLISM, and ADHERENS_JUNCTION (Fig. 3G); AQP9 was enriched in FOCAL_ADHESION, BUTANOATE_METABOLISM, and CHRON-IC_MYELOID_LEUKEMIA signaling pathways (Fig. 3H); CH25H was enriched in B_CELL_RECEPTOR_SIGNALING_PATHWAY, RETI-NOL_METABOLISM, and FOCAL_ADHESION (Fig. 3I); and PEX19 was enriched in OXIDATIVE_PHOSPHORYLATION, BETA_ALANINE_METABOLISM, and other signaling pathways (Fig. 3J). These findings indicate that the key genes may influence disease progression via modulation of these signaling pathways.

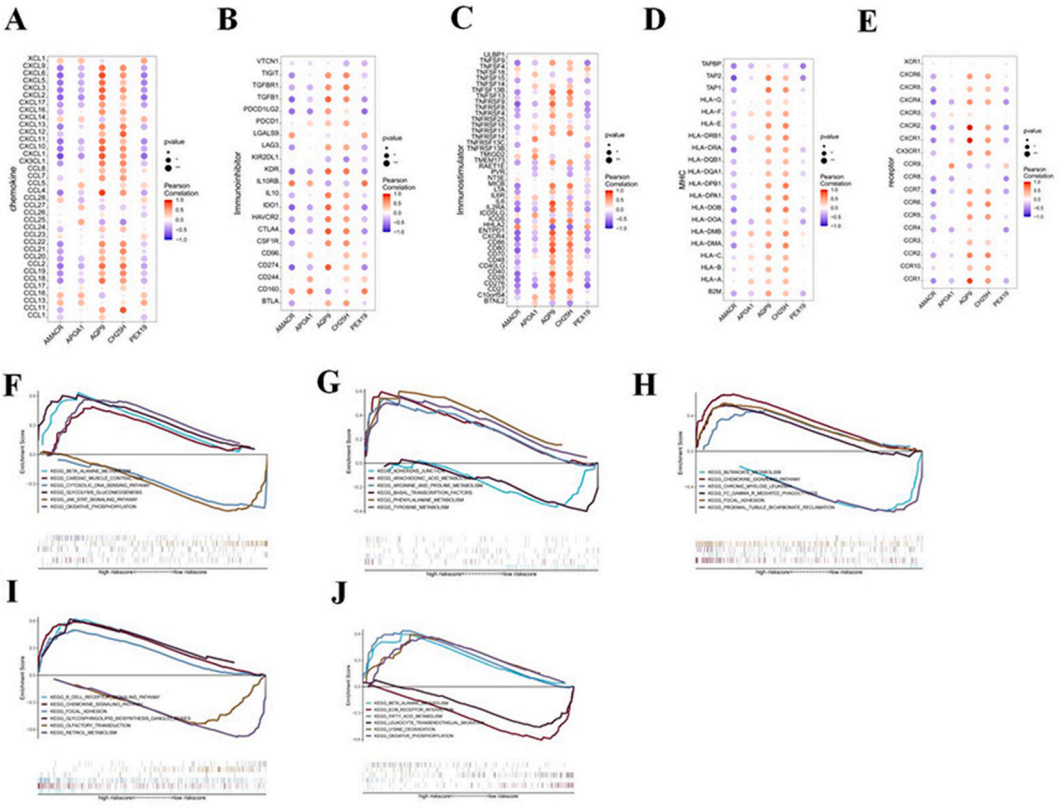

Fig. 3. The correlation between these five key genes and different immune factors as well as the specific signaling pathways involved in these genes. A: Immune related chemokines; B: Immunosuppressants; C: Immune stimulating factors; D: MHC; E: Immune related receptors; F: AMACR; G: APOA1; H: AQP9; I: CH25H; J: PEX19.

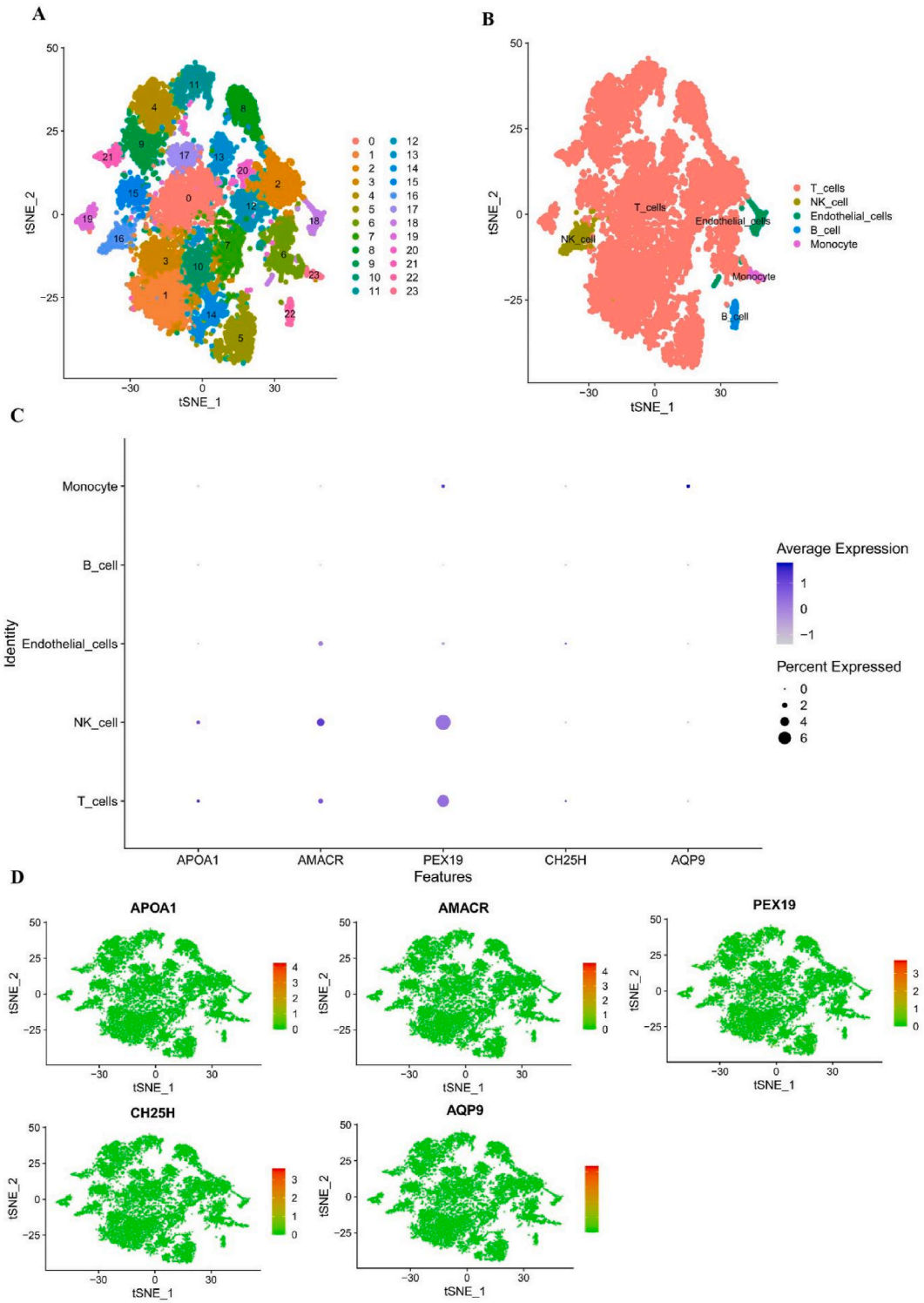

Fig. 4. The single-cell data of GSE134649 and performed single-cell analysis. A: 24 subtypes through TSNE; B: Each cluster through the R package SingleR; C–D: The expression of key genes in T_cells, NK_cell, Endothelial_cells, B_cell, and Monocyte cells.

3.4. The disease genes associated with UC

Next, the genes associated with UC were obtained from the GeneCards database (https://www.genecards.org/) [24]. The expression levels of the top 20 genes were assessed based on relevance scores and differential expression among disease-related genes was examined in various groups. Notably, significant differential expression were observed for NOD2, IL6, IL10, TNF, H19, IL23R, IL1B, TLR4, HLA-DRB1, TGFB1, IL10RA, ABCB1, TLR2, IL1RN, HLA-B, IL2, and IFNG among the groups **(Supplementary Figure).**

3.5. Single-cell analysis of UC

Single-cell data were downloaded from GSE134649 and single-cell analysis was conducted using the Seurat package. Cells were clustered using the t-SNE algorithm, resulting in 24 subtypes (Fig. 4A). Subsequently, each cluster was annotated using the SingleR package in R, which categorized all clusters into five main cell types: T_cells, NK_cells, Endothelial_cells, B_cells, and Monocytes (Fig. 4B). The expression patterns of key genes across these cell types are presented in Fig. 4C–D. AQP9 exhibited a strong association with the $CD8^+$ T cell-related gene cytotoxic T-lymphocyte-associated protein 4 (CTLA4), which was further correlated with PRDM1. APOA1 demonstrated a correlation with programmed cell death protein 1 (PDCD1) and cluster of differentiation 8 subunit beta (CD8B), while CH25H was correlated with eomesodermin (EOMES) and inducible costimulator (ICOS). All these factors positively correlated with disease progression. Similarly, AQP9 was closely associated with NK cell marker factors granzyme B (GZMB), interleukin-15 receptor subunit alpha (IL-15RA), and signal transducer and activator of transcription 1-alpha/beta (STAT1/A/B), while CH25H was strongly linked to EOMES and STAT4. All these factors positively influenced disease progression.

3.6. AQP9 inhibited the CD8+T cell activity

To validate the bioinformatics analysis findings, we isolated total RNA and protein from animal UC tissues and control tissues. Western blot and RT-PCR analysis were conducted to assess the protein expression (Fig. 5A) and messenger RNA (mRNA) (Fig. 5B) of the aforementioned five genes. The results revealed a significant upregulation of AMACR, PEX19, AQP9, and CH25H in UC tissues compared with the control group ($P < 0.05$), with AQP9 exhibiting the most profound increase. Conversely, APOA1 expression was markedly downregulated.

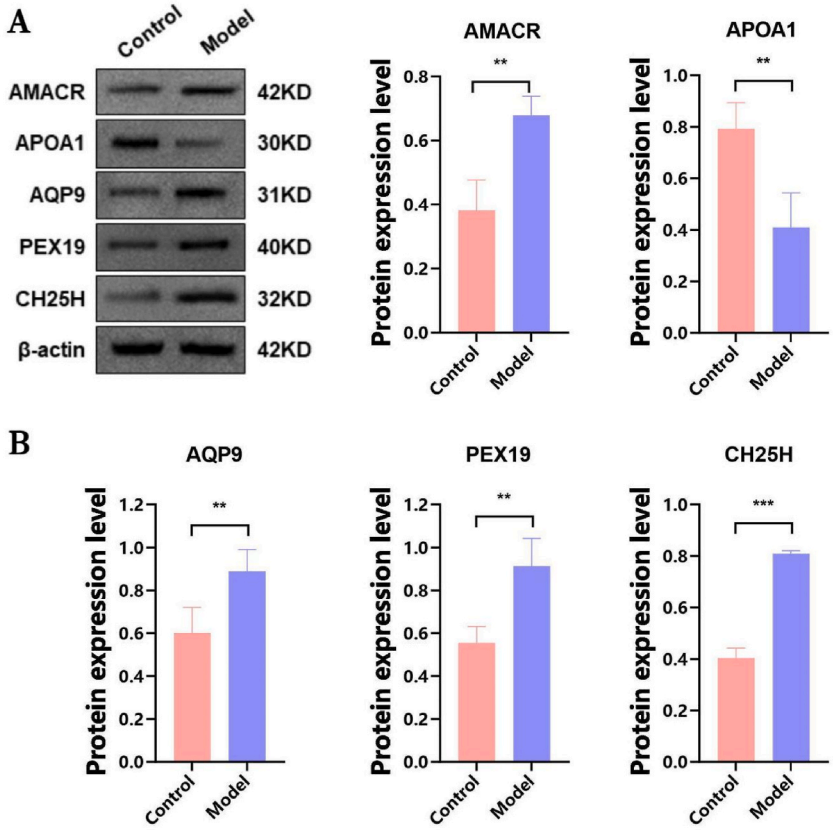

Fig. 5. The key genes expression in UC tissue. A: The protein level in UC and the gray level; B: The mRNA level of the UC. $^{**}P < 0.01$ versus control group; $^{***}P < 0.001$ versus control group.

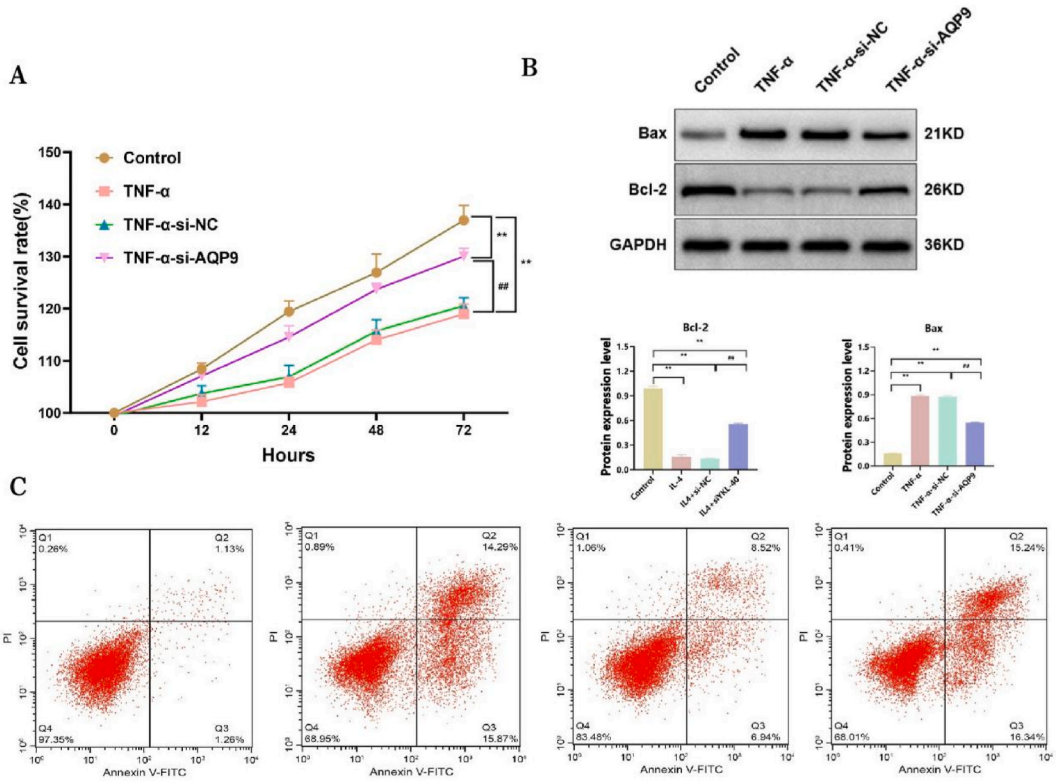

Fig. 6. Cell level analysis of the effect of AQP9 expression on CD8+T cell. A: Detection of cell activity 72 h after knocking down AQP9; B: The protein expression of apoptosis related proteins Bax and Bcl2 after knocking down AQP9; C: Flow cytometry was used to detect the apoptosis rate of cells after knocking down AQP9. $^{**}P < 0.01$ versus control group; $\#\#P < 0.01$ versus TNF-α-si-NC group.

Additionally, the infiltration of $CD8^+$ T cells has been implicated in the progression of UC, and this research further confirms the association between the AQP9 gene and $CD8^+$ T cell infiltration at cellular level (Fig. 6A). We evaluated the functionality of CD8+T cell following the knockdown of AQP9 in a TNF-α-induced cell model. TNF-α treatment substantially increased the expression of AQP9 mRNA and protein, decreased CD8+T cell activity, upregulated apoptosis-related protein Bax, downregulated Bcl2 (Fig. 6B), and elevated the cell apoptosis rate (Fig. 6C). These observations align with the bioinformatics findings. However, the cell activity partially recovered, reaching approximately 80 % of the control group after 72 h, Bax expression decreased to approximately 60 %, and Bcl2 expression was significantly upregulated after AQP9 knockdown. This led to a decrease in the cell apoptosis rate, indicating a substantial improvement effect.

3.7. AQP9 regulates CD8+T cell infiltration

The aforementioned results confirmed a strong correlation between the AQP9 and CD8+T cell. The infiltration of $CD8^+$ T cells has been implicated in the progression of UC. Our study showed that the mRNA and protein expression of AQP9 were significantly increased in CD8+T cell In the TNFα induced cellular UC model. Specifically, the CD8+T cell regulator IFN-γ and the common pathway protein JAK levels were increased remarkably following TNFα stimulation (Fig. 7A–B). These findings indicated that AQP9 may play a role in modulating the IFN-γ/JAK signaling pathway to increase the CD8+T cell infiltraion.

A knockdown efficiency of 60 % was achieved during the construction of the AQP9 knockdown short hairpin RNA (shRNA) and Lipo2000 transfected CD8+T cell model (details showed in Fig. 7C). It was found that knocking down AQP9 knockdown significantly reduced the levels of inflammatory factors IL-4 and IL-6 (which were related to CD8+T cell activity) (Fig. 7D). Which indicated that AQP9 could increase inflammatory infiltration of $CD8^+$ T cells and potentially influencing the progression of UC, AQP9 knockdown reversed this trend.

4. Discussion

The present study identified BAM and immune response as crucial mechanisms underlying the pathogenesis of UC. BAs, prevalent metabolites produced by the gut microbiota, serve as signaling molecules that modulate an individual's predisposition to intestinal inflammation. Additionally, BAs play a pivotal role in maintaining innate immunity [25,26]. BA can regulate the function of intestinal immune cells, maintain immune tolerance, and ultimately prevent the occurrence of intestinal inflammatory reactions [27].

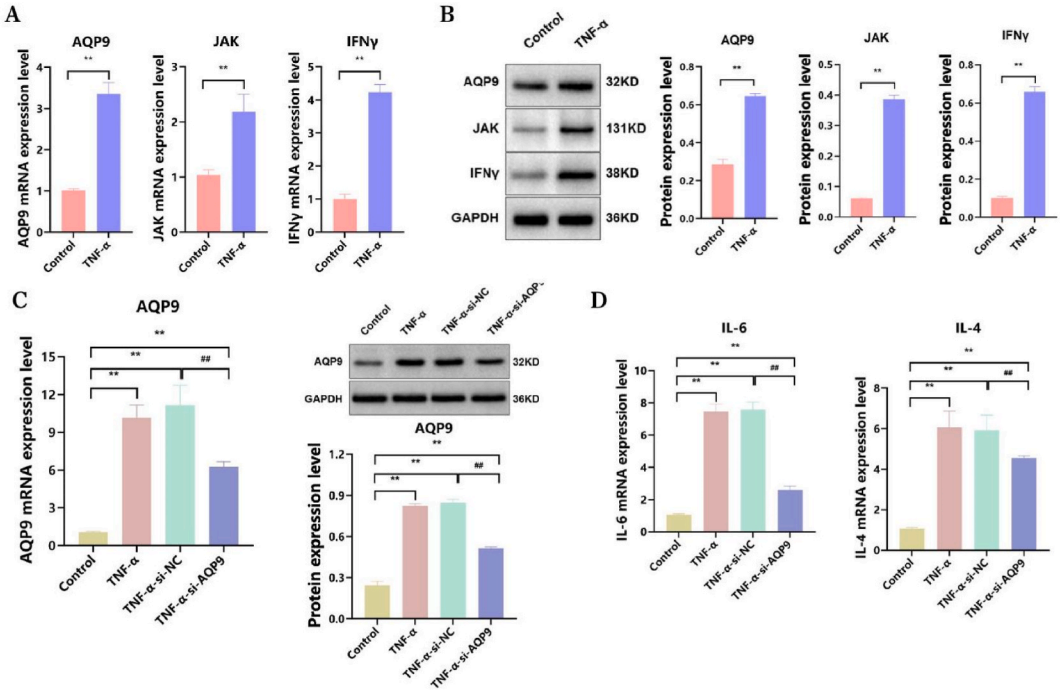

Fig. 7. The expression of the AQP9 and CD8+cell infiltration related pathway. A: The mRNA level of AQP9 and CD8+cell infiltration related protein; B: The protein level of AQP9 and CD8+cell infiltration related protein; C: AQP9 knockdown efficiency; D: The levels of CD8+T related cytokines IL-4 and IL-6. $^{**}P < 0.01$ versus control group; $\#\#P < 0.01$ versus TNF-α-si-NC group.

Dysfunctional BA signaling may contribute to immune dysregulation in UC [28]. The expression of BA inducible (bai) genes in UC tissues is significantly reduced [29].

Five overlapping BA genes (APOA1, AMACR, PEX19, CH25H, and AQP9) were identified as key genes for subsequent studies using the SVM-RFE algorithm evaluation combined with the LASSO regression algorithm. Our study sought to investigate the potential molecular mechanisms through which key genes and their correlation with immune infiltration influence UC progression. Our findings revealed that plasma cells, activated memory $CD4^+$ T cells, NK cells (resting), M0 macrophages, M1 macrophages, activated DCs, activated mast cells, and neutrophils were significantly elevated in UC patients compared with normal patients. Additionally, These five key genes are strongly correlated with immune cells and play a crucial role in the immune microenvironment. Specifically, (1) downregulation of APOA1 gene expression is negatively correlated with UC progression [30]. APOA1 mimetic has been shown to alleviate cyclooxygenase-2 (COX2) dependent intestinal inflammation [31]. APOA1 correlated with the infiltration of $CD8^+$ T cells in pediatric patients with Crohn's disease [32]. (2) AMACR can promote abnormal epithelial proliferation in UC [33]; however, no specific studies have explored its association with UC progression. To the best of our knowledge, this is the first study to reveal a direct relationship between AMACR expression and UC, providing insights into its regulatory role in immunity. (3) PEX19 can induce viruses to evade immune responses [34]. There are limited reports on its role in intestinal diseases. This study found for the first time that overexpression of PEX19 is closely related to the progression of UC. (4) CH25H exacerbated the inflammatory response of lipid-laden macrophages through modulation of cholesterol accessibility in the plasma membrane, resulting in altered Toll-like receptor 4 (TLR4) signaling, enhanced nuclear factor-κB-mediated proinflammatory gene expression, and heightened susceptibility to apoptosis [35]. The expression of CH25H mRNA was elevated in the inflamed colon of UC patients [36]. However, the underlying molecular mechanisms by which CH25H regulates UC progression are complex and deserve further exploration. (5) AQP9, an aquaporin, is involved in fluid metabolism in various epithelial and endothelial tissues. Additionally, AQP9 is implicated in cell proliferation, migration, and apoptosis, and serves as an immune-related marker that modulates tissue-specific physiological characteristics in UC tight junctions [37,38]. Previous studies reported that AQP9 expression was positively correlated with regulatory T cells, macrophage M2, $CD4^+$ T cells, and neutrophils and negatively correlated with mast cells, NK cells, and CD8+T cells [39]. Given the strong association between AQP9 and intestinal inflammation, exploring its interaction with immune mechanisms and its influence on the advancement of UC is imperative. The current study found that target genes (APOA1, AMACR, PEX19, CH25H, and AQP9) were related to BAM in UC and played a crucial role in regulating immune responses.

After further analysis, AQP9 was selected as the validation target, and the potential mechanism and principle governing AQP9 gene regulation in immune cells were elucidated at the cellular level. The UC microenvironment is primarily composed of a complex interplay of immune cells, extracellular matrix, various growth factors, inflammatory cytokines, and distinct physicochemical characteristics, all of which significantly impact the diagnosis, prognosis, and responsiveness to clinical treatments. Immune cells rely on fatty acids to regulate internal metabolic pathways, thereby maintaining normal cellular function. CD8+effector T cells associated

with UC can promote the release of TNF - α and initiate tissue damage. This study suggests that overexpression of AQP9 can promote the activation of CD8+T cells., whereas effector post cells acquire innate properties to perform regulatory functions that could potentially alleviate excessive inflammation [40]. IFN-γ-producing $CD8^+$ tissue-resident memory T cells have been identified as markers for immune checkpoint inhibitor-induced colitis [41]. Treatment with immune checkpoint inhibitors leads to $CD8^+$ T cell infiltration in patients with colitis, exhibiting a similar infiltration pattern to that observed in UC [42]. AQP9 plays a role in recruitment of $CD8^+$ T cells within the tumor microenvironment (TME), potentially hindering immune activity in the TME [43]. However, there is currently a paucity of research examining the role of AQP9 in regulating UC.

Subsequently, we further investigated the potential mechanism of AQP9 and $CD8^+$ T cell infiltration in UC cell models. Our findings showed that AQP9 enhanced IFN-γ production and stimulated the activation of $CD8^+$ T cells by modulating the JAK pathway. However, AQP9 knockdown reversed this trend. The JAK-STAT pathway, which involves JAKs and STATs, plays a crucial role in both innate and adaptive immunity [44]. Activating JAK-STAT can promote the progression of UC [45]. Research has shown that the JAK-STAT pathway is the main signaling axis that affects the formation and maintenance of memory T cells. STAT3 activation can protect the production of CD8+T cells in memory [46]. Manipulation of the JAK/STAT5 pathway has been shown to regulate $CD8^+$ T cell immune infiltration in mouse models of colitis [47]. Taken together, these findings suggest that AQP9 may promote IFN-γ production, activate the JAK signaling pathway, and sensitize $CD8^+$ T cells, ultimately contributing to the progression of UC.

In summary, this study screened and identified five BA-associated DEGs (APOA1, AMACR, PEX19, CH25H, and AQP9) that demonstrated strong correlation with immune-related DEGs. Notably, all five genes were significantly upregulated or downregulated in immune cells. Our wet experiments revealed that AQP9 plays a role in regulating JAK–IFN–γ activation of $CD8^+$ T cells, ultimately contributing to UC progression. This study provides more insights into the pathogenesis of BAM in the immune cells of UC patients and will aid in elucidating immune-related signaling pathways through genome-wide screening of pivotal genes. These discoveries offer potential theoretical targets for future clinical interventions.

Funding

This work is supported by Jiangsu Province Traditional Chinese Medicine Technology Development Plan Project (MS2023099); Natural Science Foundation of Nanjing University of Traditional Chinese Medicine (XZR2023076); Suzhou Science and Technology Bureau's "Science and Education Revitalization of Health" Youth Science and Technology Project (KJXW2023069); Changshu Science and Technology Bureau Medical Application Basic Research Project (CY202340); Changshu Health Commission Science and Technology Plan Project (CSWS202103).

Ethics approval and consent to participate

All animal experiments were performed according to the Guide for the Care and Use of Laboratory Animals, and approved by the ethical committee of Changshu Hospital Affiliated to Nanjing University of Chinese Medicine (NO.2023021).

Data availability

The datasets used and analyzed during the current study are available from the corresponding authors on reasonable request.

CRediT authorship contribution statement

Hua Huang: Writing – review & editing, Writing – original draft, Software, Resources, Project administration, Formal analysis, Data curation, Conceptualization. **Shuai Yan:** Writing – original draft, Supervision, Software, Resources, Formal analysis, Data curation, Conceptualization. **Tianwei Guo:** Writing – original draft, Project administration, Methodology, Investigation. **Qiuwen Hua:** Software, Resources, Project administration, Methodology, Investigation, Funding acquisition. **Yongtong Wang:** Visualization, Supervision, Formal analysis. **Shanshan Xu:** Writing – review & editing, Writing – original draft, Methodology, Data curation, Conceptualization. **Lijiang Ji:** Writing – review & editing, Supervision, Investigation, Funding acquisition.

Declaration of competing interest

The authors declare that they have no known competing financial interests or personal relationships that could have appeared to influence the work reported in this paper.

Acknowledgements

Not applicable.

Appendix A. Supplementary data

Supplementary data to this article can be found online at https://doi.org/10.1016/j.heliyon.2024.e34352.

References

[1] T. Raine, S. Bonovas, J. Burisch, T. Kucharzik, M. Adamina, V. Annese, O. Bachmann, D. Bettenworth, M. Chaparro, W. Czuber-Dochan, P. Eder, P. Ellul, C. Fidalgo, G. Fiorino, P. Gionchetti, J.P. Gisbert, H. Gordon, C. Hedin, S. Holubar, M. Iacucci, K. Karmiris, K. Katsanos, U. Kopylov, P.L. Lakatos, T. Lytra, I. Lyutakov, N. Noor, G. Pellino, D. Piovani, E. Savarino, F. Selvaggi, B. Verstockt, A. Spinelli, Y. Panis, G. Doherty, ECCO guidelines on therapeutics in ulcerative colitis: medical treatment, J Crohns Colitis 16 (1) (2022) 2–17.

[2] B. Gros, G.G. Kaplan, Ulcerative colitis in adults: a review, JAMA 330 (10) (2023) 951–965.

[3] L. Du, C. Ha, Epidemiology and pathogenesis of ulcerative colitis, Gastroenterol. Clin. N. Am. 49 (4) (2020) 643–654.

[4] L.E. Targownik, E.I. Benchimol, C.N. Bernstein, H. Singh, A. Tennakoon, A.A. Zubieta, S. Coward, J. Jones, G.G. Kaplan, M.E. Kuenzig, S.K. Murthy, G. C. Nguyen, J.N. Peña-Sánchez, Combined biologic and immunomodulatory therapy is superior to monotherapy for decreasing the risk of inflammatory bowel disease-related complications, J Crohns Colitis 14 (10) (2020) 1354–1363.

[5] Y. Guo, Y. Li, Q. Cao, L. Ye, J. Wang, M. Guo, The function of natural polysaccharides in the treatment of ulcerative colitis, Front. Pharmacol. 13 (2022) 927855.

[6] F. Li, J. Ouyang, Z. Chen, Z. Zhou, J. Milon Essola, B. Ali, X. Wu, M. Zhu, W. Guo, X.J. Liang, Nanomedicine for T-cell mediated immunotherapy, Adv. Mater. 25 (2023) e2301770.

[7] C. Cheng, J. Hu, Y. Li, Y. Ji, Z. Lian, R. Au, F. Xu, W. Li, H. Shen, L. Zhu, Qing-Chang-Hua-Shi granule ameliorates DSS-induced colitis by activating NLRP6 signaling and regulating Th17/Treg balance, Phytomedicine 107 (2022) 154452.

[8] P. Behzadi, A.S. Sameer, S. Nissar, M.Z. Banday, M. Gajdács, H.A. García-Perdomo, K. Akhtar, M. Pinheiro, P. Magnusson, M. Sarshar, C. Ambrosi, The interleukin-1 (IL-1) superfamily cytokines and their single nucleotide polymorphisms (SNPs), J. Immunol. Res. 2022 (2022) 2054431.

[9] S. Mukherjee, R. Patra, P. Behzadi, A. Masotti, A. Paolini, M. Sarshar, Toll-like receptor-guided therapeutic intervention of human cancers: molecular and immunological perspectives, Front. Immunol. 14 (2023) 1244345.

[10] L. Thoo, M. Noti, P. Krebs, Keep calm: the intestinal barrier at the interface of peace and war, Cell Death Dis. 10 (11) (2019) 849.

[11] C. Campbell, P.T. McKenney, D. Konstantinovsky, O.I. Isaeva, M. Schizas, J. Verter, C. Mai, W.B. Jin, C.J. Guo, S. Violante, R.J. Ramos, J.R. Cross, K. Kadaveru, J. Hambor, A.Y. Rudensky, Bacterial metabolism of bile acids promotes generation of peripheral regulatory T cells, Nature 581 (7809) (2020) 475–479.

[12] X. Song, X. Sun, S.F. Oh, M. Wu, Y. Zhang, W. Zheng, N. Geva-Zatorsky, R. Jupp, D. Mathis, C. Benoist, D.L. Kasper, Microbial bile acid metabolites modulate gut RORγ(+) regulatory T cell homeostasis, Nature 577 (7790) (2020) 410–415.

[13] G. Sorrentino, A. Perino, E. Yildiz, G. El Alam, M. Bou Sleiman, A. Gioiello, R. Pellicciari, K. Schoonjans, Bile acids signal via TGR5 to activate intestinal stem cells and epithelial regeneration, Gastroenterology 159 (3) (2020) 956–968.e958.

[14] M.E. Ritchie, B. Phipson, D. Wu, Y. Hu, C.W. Law, W. Shi, G.K. Smyth, Limma powers differential expression analyses for RNA-sequencing and microarray studies, Nucleic Acids Res. 43 (7) (2015) e47.

[15] X. Hu, S. Ni, K. Zhao, J. Qian, Y. Duan, Bioinformatics-led discovery of osteoarthritis biomarkers and inflammatory infiltrates, Front. Immunol. 13 (2022) 871008.

[16] Ali Amer A. Youssef, Global-local least-squares support vector machine (GLocal-LS-SVM), PLoS One 18 (4) (2023) e0285131.

[17] W. Zhong, T. Darville, X. Zheng, J. Fine, Y. Li, Generalized multi-SNP mediation intersection-union test, Biometrics 78 (1) (2022) 364–375.

[18] B. Chen, M.S. Khodadoust, C.L. Liu, A.M. Newman, A.A. Alizadeh, Profiling tumor infiltrating immune cells with CIBERSORT, Methods Mol. Biol. 1711 (2018) 243–259.

[19] K. Krug, P. Mertins, B. Zhang, et al., A curated resource for phosphosite-specific signature analysis, Mol. Cell. Proteomics 18 (3) (2019) 576–593.

[20] S. Aibar, C.B. González-Blas, T. Moerman, V.A. Huynh-Thu, H. Imrichova, G. Hulselmans, F. Rambow, J.C. Marine, P. Geurts, J. Aerts, J. van den Oord, Z. K. Atak, J. Wouters, S. Aerts Scenic, single-cell regulatory network inference and clustering, Nat. Med. 14 (11) (2017) 1083–1086.

[21] Y. Hao, S. Hao, E. Andersen-Nissen, W.M. Mauck 3rd, S. Zheng, A. Butler, M.J. Lee, A.J. Wilk, C. Darby, M. Zager, P. Hoffman, M. Stoeckius, E. Papalexi, E. P. Mimitou, J. Jain, A. Srivastava, T. Stuart, L.M. Fleming, B. Yeung, A.J. Rogers, J.M. McElrath, C.A. Blish, R. Gottardo, P. Smibert, R. Satija, Integrated analysis of multimodal single-cell data, Cell 184 (13) (2021) 3573–3587.e3529.

[22] X. Wang, G. Chen, L. Nie, Z. Wu, X. Wang, C. Pan, X. Chen, X. Zhao, J. Zhu, Q. He, H. Wang, IL-2K35C-moFA, a long-acting engineered cytokine with decreased interleukin 2 receptor α binding, improved the cellular selectivity profile and antitumor efficacy in a mouse tumor model, Cancers 14 (19) (2022) 4742.

[23] B. Ru, C.N. Wong, Y. Tong, J.Y. Zhong, S.S.W. Zhong, W.C. Wu, K.C. Chu, C.Y. Wong, C.Y. Lau, I. Chen, N.W. Chan, J. Zhang, TISIDB: an integrated repository portal for tumor-immune system interactions, Bioinformatics 35 (20) (2019) 4200–4202.

[24] G. Stelzer, N. Rosen, I. Plaschkes, S. Zimmerman, M. Twik, S. Fishilevich, T.I. Stein, R. Nudel, I. Lieder, Y. Mazor, S. Kaplan, D. Dahary, D. Warshawsky, Y. Guan-Golan, A. Kohn, N. Rappaport, M. Safran, D. Lancet, The GeneCards suite: from gene data mining to disease genome sequence analyses, Curr. Protoc. Bioinformatics 54 (2016) 1–30.

[25] F. Kuipers, J.F. de Boer, B. Staels, Microbiome modulation of the host adaptive immunity through bile acid modification, Cell Metabol. 31 (3) (2020) 445–447.

[26] J. Cai, L. Sun, F.J. Gonzalez, Gut microbiota-derived bile acids in intestinal immunity, inflammation, and tumorigenesis, Cell Host Microbe 30 (3) (2022) 289–300.

[27] J. Cai, B. Rimal, C. Jiang, J.Y.L. Chiang, A. D. Patterson Bile acid metabolism and signaling, the microbiota, and metabolic disease, Pharmacol. Therapeut. 237 (2022) 108238.

[28] S.R. Sinha, Y. Haileselassie, L.P. Nguyen, C. Tropini, M. Wang, L.S. Becker, D. Sim, K. Jarr, E.T. Spear, G. Singh, H. Namkoong, K. Bittinger, M.A. Fischbach, J. L. Sonnenburg, A. Habtezion, Dysbiosis-induced secondary bile acid deficiency promotes intestinal inflammation, Cell Host Microbe 27 (4) (2020) 659–670.

[29] X. Liu, Y. Zhang, W. Li, B. Zhang, J. Yin, S. Liuqi, J. Wang, B. Peng, S. Wang, Fucoidan ameliorated dextran sulfate sodium-induced ulcerative colitis by modulating gut microbiota and bile acid metabolism, J. Agric. Food Chem. 70 (47) (2022) 14864–14876.

[30] M. Blaschke, R. Koepp, C. Lenz, J. Kruppa, K. Jung, H. Siggelkow, Crohn's disease patient serum changes protein expression in a human mesenchymal stem cell model in a linear relationship to patients' disease stage and to bone mineral density, J. Clin. Transl. Endocrinol. 13 (2018) 26–38.

[31] D. Meriwether, D. Sulaiman, C. Volpe, A. Dorfman, V. Grijalva, N. Dorreh, R.S. Solorzano-Vargas, J. Wang, E. O'Connor, J. Papesh, M. Larauche, H. Trost, M. N. Palgunachari, G.M. Anantharamaiah, H.R. Herschman, M.G. Martin, A.M. Fogelman, S.T. Reddy, Apolipoprotein A-I mimetics mitigate intestinal inflammation in COX2-dependent inflammatory bowel disease model, J. Clin. Invest. 129 (9) (2019) 3670–3685.

[32] S. Xiao, W. Xie, Y. Zhang, Y. Pan, L. Lei, The immune landscape and molecular subtypes of pediatric crohn's disease: results from in silico analysis, J. Personalized Med. 13 (4) (2023) 571.

[33] R. Dorer, R.D. Odze, AMACR immunostaining is useful in detecting dysplastic epithelium in Barrett's esophagus, ulcerative colitis, and Crohn's disease, Am. J. Surg. Pathol. 30 (7) (2006) 871–877.

[34] G. Anuraga, J. Lang, D.T.M. Xuan, H.D.K. Ta, J.Z. Jiang, Z. Sun, S. Dey, S. Kumar, A. Singh, G. Kajla, W.J. Wang, C.Y. Wang, Integrated bioinformatics approaches to investigate alterations in transcriptomic profiles of monkeypox infected human cell line model, J Infect Public Health 17 (1) (2024) 60–69.

[35] A. Canfrán-Duque, N. Rotllan, X. Zhang, I. Andrés-Blasco, B.M. Thompson, J. Sun, N.L. Price, M. Fernández-Fuertes, J.W. Fowler, D. Gómez-Coronado, W. C. Sessa, C. Giannarelli, R.J. Schneider, G. Tellides, J.G. McDonald, C. Fernández-Hernando, Y. Suárez, Macrophage-derived 25-hydroxycholesterol promotes vascular inflammation, atherogenesis, and lesion remodeling, Circulation 147 (5) (2023) 388–408.

[36] A. Wyss, T. Raselli, N. Perkins, F. Ruiz, G. Schmelczer, G. Klinke, A. Moncsek, R. Roth, M.R. Spalinger, L. Hering, K. Atrott, S. Lang, I. Frey-Wagner, J.C. Mertens, M. Scharl, A.W. Sailer, O. Pabst, M. Hersberger, C. Pot, G. Rogler, B. Misselwitz, The EBI2-oxysterol axis promotes the development of intestinal lymphoid structures and colitis, Mucosal Immunol. 12 (3) (2019) 733–745.

[37] Q. Cheng, J. Zhang, H. Ding, Z. Wang, J. Fang, X. Fang, M. Li, R. Li, J. Meng, H. Liu, X. Lu, Y. Xu, C. Chen, W. Zhang, Integrated multiomics analysis reveals changes in liver physiological function in Aqp9 gene knockout mice, Int. J. Biol. Macromol. 245 (2023) 125459.

[38] H. Taman, C.G. Fenton, I.V. Hensel, E. Anderssen, J. Florholmen, R.H. Paulssen, Transcriptomic landscape of treatment-naïve ulcerative colitis, J. Crohns Colitis. 12 (3) (2018) 327–336.

[39] J. Jing, J. Sun, Y. Wu, N. Zhang, C. Liu, S. Chen, W. Li, C. Hong, B. Xu, M. Chen, AQP9 is a prognostic factor for kidney cancer and a promising indicator for M2 TAM polarization and CD8+ T-cell recruitment, Front. Oncol. 11 (2021) 770565.
[40] D. Corridoni, A. Antanaviciute, T. Gupta, D. Fawkner-Corbett, A. Aulicino, M. Jagielowicz, K. Parikh, E. Repapi, S. Taylor, D. Ishikawa, R. Hatano, T. Yamada, W. Xin, H. Slawinski, R. Bowden, G. Napolitani, O. Brain, C. Morimoto, H. Koohy, A. Simmons, Single-cell atlas of colonic CD8(+) T cells in ulcerative colitis, Nat. Med. 26 (9) (2020) 1480–1490.
[41] S.C. Sasson, S.M. Slevin, V.T.F. Cheung, I. Nassiri, A. Olsson-Brown, E. Fryer, R.C. Ferreira, D. Trzupek, T. Gupta, L. Al-Hillawi, M.L. Issaias, A. Easton, L. Campo, M.E.B. FitzPatrick, J. Adams, M. Chitnis, A. Protheroe, M. Tuthill, N. Coupe, A. Simmons, M. Payne, M.R. Middleton, S.P.L. Travis, B.P. Fairfax, P. Klenerman, O. Brain, Interferon-gamma-producing CD8(+) tissue resident memory T cells are a targetable hallmark of immune checkpoint inhibitor-colitis, Gastroenterology 161 (4) (2021) 1229–1244.
[42] S. Hone Lopez, G. Kats-Ugurlu, R.J. Renken, H.J. Buikema, M.R. de Groot, M.C. Visschedijk, G. Dijkstra, M. Jalving, J.J. de Haan, Immune checkpoint inhibitor treatment induces colitis with heavy infiltration of CD8 + T cells and an infiltration pattern that resembles ulcerative colitis, Virchows Arch. 479 (6) (2021) 1119–1129.
[43] J. Jing, J. Sun, Y. Wu, N. Zhang, C. Liu, S. Chen, W. Li, C. Hong, B. Xu, M. Chen, AQP9 is a prognostic factor for kidney cancer and a promising indicator for M2 TAM polarization and CD8+ T-cell recruitment, Front. Oncol. 11 (2021) 770565.
[44] Q. Hu, Q. Bian, D. Rong, L. Wang, J. Song, H.S. Huang, J. Zeng, J. Mei, P.Y. Wang, JAK/STAT pathway: extracellular signals, diseases, immunity, and therapeutic regimens, Front. Bioeng. Biotechnol. 11 (2023) 1110765.
[45] S. van Gennep, I.C.N. Fung, D.C. de Jong, R.K. Ramkisoen, E. Clasquin, J. de Jong, L.C.S. de Vries, W.J. de Jonge, K.B. Gecse, M. Löwenberg, J.C. Woolcott, A. Mookhoek, G.R. D'Haens, Histological outcomes and jak-stat signalling in ulcerative colitis patients treated with tofacitinib, J Crohns Colitis (2024), https://doi.org/10.1093/ecco-jcc/jjae031.
[46] Y. Wang, F. Qiu, Y. Xu, X. Hou, Z. Zhang, L. Huang, H. Wang, H. Xing, S. Wu, Stem cell-like memory T cells: the generation and application, J. Leukoc. Biol. 110 (6) (2021) 1209–1223.
[47] M. Wang, X. Huang, Z. Kang, J. Huang, S. Wei, H. Zhao, Y. Zhong, D. Liu, Mechanism of sishen-pill-regulated special memory T and mTfh cell via involving JAK/STAT5 pathway in colitis mice, Evid. Based Complement. Altern. Med. 2022 (2022) 6446674.